Development/Plasticity/Repair

Perlecan Antagonizes Collagen IV and ADAMTS9/GON-1 in Restricting the Growth of Presynaptic Boutons

Jianzhen Qin,[1,2] **Jingjing Liang,**[1] **and Mei Ding**[1]

[1]State Key Laboratory of Molecular Developmental Biology, Institute of Genetics and Developmental Biology, Chinese Academy of Sciences, Beijing 100101, China, and [2]University of Chinese Academy of Sciences, Beijing 100049, China

In the mature nervous system, a significant fraction of synapses are structurally stable over a long time scale. However, the mechanisms that restrict synaptic growth within a confined region are poorly understood. Here, we identified that in the *C. elegans* neuromuscular junction, collagens Type IV and XVIII, and the secreted metalloprotease ADAMTS/GON-1 are critical for growth restriction of presynaptic boutons. Without these components, ectopic boutons progressively invade into the nonsynaptic region. Perlecan/UNC-52 promotes the growth of ectopic boutons and functions antagonistically to collagen Type IV and GON-1 but not to collagen XVIII. The growth constraint of presynaptic boutons correlates with the integrity of the extracellular matrix basal lamina or basement membrane (BM), which surrounds chemical synapses. Fragmented BM appears in the region where ectopic boutons emerge. Further removal of UNC-52 improves the BM integrity and the tight association between BM and presynaptic boutons. Together, our results unravel the complex role of the BM in restricting the growth of presynaptic boutons and reveal the antagonistic function of perlecan on Type IV collagen and ADAMTS protein.

Key words: **ADAMTS9/GON-1; basement membrane; perlecan/UNC-52; presynaptic boutons; Type IV collagen/EMB-9; Type XVIII collagen/CLE-1**

Introduction

Synapses are specialized intercellular junctions between neurons or between neurons and other excitable cells. The presynaptic plasma membrane is characterized by a cluster of neurotransmitter-filled synaptic vesicles, whereas the postsynaptic membrane contains an accumulation of neurotransmitter receptors. The intercellular space between these two membranes is named the synaptic cleft. At central synapses, the link between the presynaptic and postsynaptic membranes is very tight. Although electron microscopy has revealed that the synaptic cleft of central synapses is filled with electron-dense material (Gray, 1959), the precise molecular nature of the material is unknown. At neuromuscular junctions (NMJs), the synaptic cleft is considerably wider and present in the form of a basal lamina or basement membrane (BM) (Palay and Chan-Palay, 1976; Burns and Augustine, 1995). The BM contains laminin and collagen IV, along with collagens Type XV and XVIII, nidogen, and heparan sulfate proteoglycans, such as perlecan and agrin. The synaptic BM is essential for proper NMJ formation. Lack of agrin leads to failure of acetylcholine receptor clustering at the postsynaptic site (Campanelli et al., 1992; Gesemann et al., 1995; Jones et al., 1997). Collagen IV can induce presynaptic differentiation (Fox et al., 2007). Loss of laminin chains results in gross NMJ abnormalities (Noakes et al., 1995; Allamand et al., 1997; Patton et al., 2001; Knight et al., 2003; Nishimune et al., 2004; Miner et al., 2006; Fox et al., 2007) or misregistration of presynaptic and postsynaptic structures (Patton et al., 2001; Ichikawa et al., 2005). Recent studies showed that collagen XVIII may contribute to synapse formation in the brain (Su et al., 2012). However, the more general role of the extracellular components in the formation of central synapses remains to be determined.

In *C. elegans*, muscle cells have long neuron-like processes (muscle arms) that run to the nerve bundles in which motor axons reside, and presynapses are observed as bulging varicosities (*en passant*) along the processes (White et al., 1986). In worms, a distinct basal lamina covers both the ventral and dorsal cords where the motor neurons are positioned (White et al., 1986). Currently, it is unclear how the presynaptic boutons are maintained within relatively confined regions of the dorsal and ventral cords. Several BM genes have been implicated in worm nervous system development. For instance, malfunction of Type XVIII collagen/CLE-1 and nidogen/NID-1 results in distinct defects in synapse organization (Ackley et al., 2003), and neuron migration

Received Dec. 8, 2013; revised June 21, 2014; accepted June 25, 2014.

Author contributions: J.Q. and M.D. designed research; J.Q. and J.L. performed research; J.Q. and M.D. analyzed data; J.Q. and M.D. wrote the paper.

This work was supported by the National Natural Science Foundation of China (31130023 and 31222026), the National Basic Program of China Grants 2014CB942803 and 2011CB965003, and Chinese Academy of Sciences (KSCX-EW-R-05). M.D. was supported by the "One Hundred Talent" project from the Chinese Academy of Sciences. We thank Dr. Shohei Mitani, Dr. Mei Zhen, Dr. William Wadsworth, Dr. David Sherwood, Dr. Myeongwoo Lee, Dr. Kang Shen, Dr. Zhaohui Wang, Dr. Xun Huang, and Mr Yunsheng Cheng for providing reagents, strains, and technical support. Monoclonal antibody MH3 was obtained from the Developmental Studies Hybridoma Bank developed under the auspices of the National Institute of Child Health and Human Development and maintained by the University of Iowa (Department of Biological Sciences, Iowa City, Iowa). Some *C. elegans* strains were provided by the Caenorhabditis Genetics Center, which is supported by the National Institutes of Health National Center for Research Resources.

The authors declare no competing financial interests.

Correspondence should be addressed to Dr. Mei Ding, Institute of Genetics and Developmental Biology, Chinese Academy of Sciences, Beijing 100101, China. E-mail: mding@genetics.ac.cn.

DOI:10.1523/JNEUROSCI.5128-13.2014

 0270-6474/14/3410311-14$15.00/0

Table 1. The roles of BM and BM-related molecules in presynaptic bouton restriction[a]

Common name	Gene	Method of depletion	Bouton growth defects
Basement membrane components			
Collagen IV α1	*emb-9*	*xd51,b189,cg46*	+
Collagen IV α2	*let-2*	*g30*	+
Collagen XVIII	*cle-1*	*cg120*	+
Fibulin-1	*fbl-1*	*tk45*	−
Hemicentin	*him-4*	*e1267*	−
Laminin αA	*lam-3*	RNAi	−
Laminin αB	*epi-1*	*gm57*	−
Laminin β	*lam-1*	*rh219*	−*
Laminin γ	*lam-2*	RNAi	−
Nidogen	*nid-1*	*cg119*	−
Osteonectin	*ost-1*	RNAi	−
Papilin	*mig-6*	*ev700*	−
Perlecan	*unc-52*	*e1421,e998*	−
Receptors of basement membrane components			
Dystroglycan	*dgn-1*	*cg121*	−
Dystroglycan	*dgn-2*	*ok209*	−
Dystroglycan	*dgn-3*	*tm1092*	−
Glypican	*gpn-1*	*ok377*	−
Glypican	*lon-2*	*e678*	−
Integrin α	*ina-1*	*gm144*	−
Integrin α	*pat-2*	RNAi	−
Integrin β	*pat-3*	*pat-3(sp)*	−*
LAR-RPTP	*ptp-3*	*ok244*	−
Syndecan	*sdn-1*	*zh20*	−
Discoidin domain receptor	*ddr-1*	*ok874*	−
Discoidin domain receptor	*ddr-2*	*ok574*	−
Slit homolog	*slt-1*	*eh15*	−
Related enzymes			
ADAMTS proteinase	*gon-1*	*e2551/q518*	+
ADAMTS proteinase	*mig-17*	*k113*	−
ADAM proteinase	*unc-71*	*e541*	−*
ADAM proteinase	*adt-1*	*cn30*	−
ADAM proteinase	*sup-17*	*n316*	−

[a] +, ectopic boutons; −, no ectopic boutons.

*Axon guidance defect.

is defective in *cle-1* mutants (Ackley et al., 2001). However, it has not been revealed whether the BM is involved in restricting presynaptic bouton growth.

Through genetic analysis, we identified that collagen Type IV, collagen Type XVIII, and ADAMTS/GON-1 are essential for restricting presynaptic bouton growth. Without these molecules, ectopic boutons emerge progressively in nonsynaptic regions. Perlecan/UNC-52 promotes ectopic bouton formation and functions antagonistically to collagen Type IV and GON-1 but not to collagen XVIII. Thus, our results provide an important link between BM and presynapse growth and reveal the antagonistic role of perlecan on selective BM components during nervous system development.

Materials and Methods

Caenorhabditis elegans *genetics.* Culture and manipulation of *C. elegans* strains were performed using standard methods (Brenner, 1974). All the strains were raised at 22°C in an HP400S biochemical incubator unless indicated otherwise. Mutants and transgenic fluorescent reporters used in these studies are listed here and in Table 1: LGI, *cle-1(cg120), sup-17(n316).* LGII, *unc-52(e998), unc-52(e1421), ptp-3(ok244), juIs76(Punc-25::GFP).* LGIII, *emb-9(b189), emb-9(xd51), emb-9(g23,cg46), ina-1(gm144), unc-71(e541),* LGIV, *fbl-1(tk45), epi-1(gm57), gon-1(e2551), gon-1(q518).* LGV, *mig-6(ev700), mig-17(k113), xdIs7 (Phmr-1b::GFP::RAB-3; Podr-1::RFP).* LGX, *let-2(g30), him-4(e1267), dgn-1(cg121), dgn-2(ok209), dgn-3(tm1092), sdn-1(zh20), ddr-1(ok874), ddr-2(ok574), slt-1(eh15), adt-1(cn30), xdIs8 (Phmr-1b::GFP::RAB-3; Podr-1::RFP).*

The genetic screen was performed according to a previous report (Song et al., 2010). Briefly, *xdIs7* animals were treated with EMS, and mutants with defective synaptic growth were isolated in the F2 generation. *xdIs7* is an integrated transgenic line of P*hmr-1b*::GFP::RAB-3 for labeling presynapses in DD, VD, and AS motor neurons. The synapse phenotype was examined at the young adult stage under a fluorescence microscope. Mutant animals were recovered to produce progeny. A total of 1800 mutagenized haploid genomes were screened.

Generation of transgenic lines and constructs. The presynaptic structures of DD, VD, and AS neurons were labeled by GFP::RAB-3 driven by 3.9 kb of *hmr-1b* upstream sequence. The *hmr-1b* promoter was inserted between the BamHI and SphI sites of the δ-pSM vector (a generous gift from Dr. Kang Shen), and GFP::RAB-3 was inserted between the NheI and HincII sites. SNB-1 cDNA was cloned into the NheI site of the P*hmr-1b*:mCherry-containing vector. To express *emb-9* in body wall muscle, a 7.6 kb *emb-9* genomic DNA fragment was cloned into the NotI and KpnI sites of the δpSM vector, and a 0.6 kb *unc-54* promoter fragment was cloned into the HindIII and SphI sites. For neuronal expression of *emb-9*, 0.4 kb of *hmr-1b* promoter was cloned into the HindIII and SphI sites of the *emb-9*-containing vector. The P*unc-25*::UNC-10::GFP marker was a kind gift from Dr. Mei Zhen. P*lam-1*::Laminin:GFP was generously provided by Dr. David Sherwood, and P*him-4*::Mb::YFP was a kind gift from Dr. Peter Roy. The P*lag-2::gon-1* was a kind gift from Dr. Shohei Mitani. In general, the plasmids were injected at 1–50 ng/μl and the coinjection markers P*odr-1*::dsRed, pRF4-*rol-6*, P*odr-1*::GFP, or P*myo-2*:RFP were injected at 10–50 ng/μl. *xdIs7* is an integrated transgenic line of P*hmr-1b*::GFP::RAB-3 and was outcrossed three times before genetic analysis.

Complementation test. For the complementation test, *emb-9(xd51); xdIs7* males were crossed with *unc-36(e251) emb-9(g23cg46)/qc1dpy-19(e1259) glp-1(q339)* hermaphrodites. Eighteen of 38 hermaphrodite progeny carrying the synaptic marker *xdIs7* displayed the ectopic bouton phenotype. In addition, *emb-9(xd51);xdIs7* males were crossed with *emb-9(b189)*, and the hermaphrodite progeny carrying *xdIs7* were scored for ectopic boutons ($n = 31$).

Quantification of presynaptic boutons. The number of ectopic presynaptic boutons along the entire dorsal nerve cord was counted in 49–180 young adults for each genotype. Only those ectopic GFP::RAB-3 puncta located outside of the dorsal nerve cord were counted. Larvae with two lines of alae (epidermal protrusions) along the lateral side were categorized as L1 stage. Larvae with a typical white vulval patch in the mid-ventral region were categorized as L4 stage. Larvae of intermediate size between L1 and L4 were categorized as L2/L3 stage. Measurements of GFP::RAB-3 and Laminin::GFP puncta were performed on confocal images as described previously (Ackley et al., 2005), and the experimenter was blind to genotype.

The codistribution of mCherry::RAB-3 and UNC-29::GFP was measured as follows. Confocal stacks were projected into a single plane. mCherry::RAB-3 puncta $>0.2\ \mu m^2$ were measured. The RAB-3/UNC-29 juxtaposition was counted as positive when at least half of the width of a mCherry::RAB-3 punctum was adjacent to the UNC-29::GFP fluorescence. Data are presented as the percentage of mCherry::RAB-3 puncta that are adjacent to UNC-29::GFP in any given defined region on the dorsal side. Only young adult animals were measured. For both presynaptic boutons and ectopic boutons, 50 mCherry::RAB-3 puncta were measured. All data are shown as mean ± SEM. Statistical analyses were performed with Student's *t* test.

RNAi experiments. For RNAi-mediated gene knockdown, *in vitro* transcription of the indicated genes was performed with TAKARA RNA polymerase. The dsRNA was microinjected into either gonad or intestine of young adults. After injection, worms were removed to NGM plates to recover for 6–7 h. The eggs laid during the first 12 h were raised at 22°C, and the synaptic phenotype was scored at the young adult stage. For

genes that are essential for viability (*lam-2*, *pat-2*, and *pat-3*) or motility (*unc-52*), the lethality or locomotion defect was examined to ensure the knockdown efficiency of RNAi treatment. RNAi primers used in this study are as follows: 5′CTCGAGCTCTCTGCTGAAATAAC3′ and 5′AGTCAGACTGGAAGTCACTGAGG3′ for *unc-52*; 5′TGCTCTCCGTACTTTTGGCT 3′ and 5′ CGAATGCTCCGATGGATACT 3′ for *lam-2*; 5′GAACTCAGGAGAGCGTGGTC for 5′TGGTTTCGGGAATCCAATAA3′ for *lam-3*; 5′ GCAGTAGAGCCAGCCAAGAAC3′ and CTGGAAGAGCCAGTCAGCCATG for *ost-1*; and 5′TTGCCAAGACACCAAATGAA and 5′AAACCGCTTCACAAAATTGG3′ for *pat-2*.

Image acquisition and statistical analysis. Animals were mounted on 2% agar in M9 buffer containing 1% 1-phenoxy-2-propanol, and fluorescence photographs were taken using a Zeiss Axioimager A1 with an AxioCam digital camera and Axiovision rel.4.6 software (Carl Zeiss) or an IX81 Olympus inverted confocal microscope. The 3D images were derived from confocal images and were processed using the Imaris 5.0 *surface* module.

The ectopic bouton phenotype on the dorsal side was classified into four groups: (1) no defect with zero extra presynaptic boutons; (2) mild with 1–2 extra presynaptic boutons; (3) intermediate with 3–9 extra presynaptic boutons; or (4) severe with ≥10 extra presynaptic boutons. *p* values were calculated by unpaired, two-tailed Student's *t* test. All statistical analyses were performed using Microsoft Excel 2010.

Immunohistochemistry. Immunohistochemistry was performed with whole-mount worms according to a previous report (Francis and Waterston, 1991). For immunofluorescence detection of endogenous UNC-52, worms were sequentially stained with the anti-UNC-52 mouse monoclonal antibody MH3, which was purchased from the Developmental Studies Hybridoma Bank. MH3 was used at 1:100 dilution. FITC-conjugated goat anti-mouse (Earthox) and DyLight 594 Affinipure goat anti-mouse (Earthox) secondary antibodies were used at 1:100 dilution. Samples were viewed with an IX81 Olympus inverted confocal microscope.

Electron microscopy and analysis. Young adult hermaphrodite animals were fixed in 2.5% glutaraldehyde, 0.8% PFA, 0.2 M cacodylate buffer for 2 h on ice. Subsequently, samples were cut and fixed in 0.5% OsO_4, 0.1 M cacodylate buffer, mounted in an agar block, dehydrated in an alcohol series, and embedded in a mixture of Embed 812. Serial sections (60 nm) were cut on a Leica UC-6, and pictures of the dorsal nerve cord near the tail were taken with a JEM-1400 electron microscope at 80 kV. Chemical presynapses were identified by the accumulation of synaptic vesicles and the appearance of darkly stained active zones. 3D EM images were constructed from 56 serial sections using the Imaris 5.0 *surface* module.

Results

Ectopic presynaptic boutons appear in *xd51* mutants

To systematically identify components that restrict presynaptic boutons to the proper location in worms, we constructed the P*hmr-1b*::GFP::RAB-3 expression line. RAB-3 is the homolog of the small GTPase Rab3, which is localized on synaptic vesicles (Fischer von Mollard et al., 1990; Mizoguchi et al., 1990). Under the control of the P*hmr-1b* promoter, this RAB-3 marker highlights presynaptic structures in VD, DD, and AS motor neurons (Broadbent and Pettitt, 2002; Mahoney et al., 2006). Within those motor neurons, this functional GFP::RAB-3 highlights punctalike synaptic vesicle clusters formed *en passant* and evenly distributed along both ventral and dorsal nerve cords (Fig. 1*A*,*B*). Because the bright GFP signal is concentrated only on the dorsal and ventral cords (Fig. 1*A*), mutants with presynapses at ectopic sites can be easily identified. Through a genetic screen with this marker, we isolated the *xd51* mutant. *xd51* animals are viable and move normally. In 95% of adult *xd51* animals, we found that some RAB-3 puncta appear at ectopic locations outside the ventral and dorsal nerve cords (Fig. 1*C*). These ectopic RAB-3 dots are comparable in size with those along the dorsal or ventral cord (~1–2 μm in diameter). To determine whether an axon guidance defect is responsible for the extra RAB-3 puncta, we examined the neuronal morphology using P*unc-25*::GFP, which highlights DD and VD neurons (Jin et al., 1999). With this marker, we found that the axons still form tight bundles along the ventral and dorsal side. In addition, the longitudinal and commissural processes show no evidence of axon guidance defects (Fig. 1*D*,*E*). However, small axonal sprouts derived from both dorsal and ventral cords emerge in *xd51* mutants (Fig. 1*F*,*G*). SNB-1 is the *C. elegans* synaptobrevin, a synaptic vesicle membrane protein involved in vesicle docking and exocytosis (Nonet, 1999). Double staining with the P*unc-25*::mCherry::SNB-1 further showed that these sprouts correlate well with ectopic boutons (Fig. 1*F*,*G*), suggesting that *xd51* may affect the proper localization of presynapses. Ectopic boutons appeared on both ventral and dorsal sides of the worm; however, the relatively small number of neuronal processes and the lack of neuron cell bodies make the dorsal cord more suitable than the ventral cord for unambiguously identifying ectopic presynaptic structures. Therefore, unless stated specifically, only the ectopic boutons on the dorsal side were scored in this study.

We next asked whether the ectopic RAB-3 puncta represent assembled presynaptic structures. We created the mCherry::SNB-1 marker under the control of the P*hmr-1*b promoter. In wild-type animals, mCherry::SNB-1 colocalizes well with P*hmr-1b*::GFP::RAB-3, suggesting that the mCherry-fused SNB-1 is functional (data not shown). When we introduced this double-labeling marker into *xd51* mutants, we found that mCherry::SNB-1 colocalized well with GFP::RAB-3 at the ectopic bouton sites (Fig. 1*H*). Furthermore, the active zone protein UNC-10/RIM (Koushika et al., 2001) driven by P*unc-25* was also detected in the region where the extra boutons formed and colocalized with P*unc-25*::mCherry::SNB-1 (Fig. 1*I*) (Koushika et al., 2001). Thus, the ectopic RAB-3 puncta in *xd51* mutants may represent assembled presynaptic structures.

Collagen Type IV is required for presynaptic bouton restriction

xd51 was mapped to chromosome III between +0.16 and +1.14, and *de novo* sequencing revealed a single nucleotide change in the *emb-9* gene. *emb-9* encodes the α1 chain of Type IV collagen (Guo et al., 1991). Nonfibril-forming Type IV collagens are shared by almost all metazoans (Hynes and Zhao, 2000; Huxley-Jones et al., 2007; Yurchenco, 2011). The most common variant consists of two α1 subunits and one α2 subunit. Each collagen IV trimer contains an N-terminal cysteine-rich domain, a long collagenous triple helical domain, and a carboxy-terminal NC1 (noncollagenous) domain (Timpl et al., 1981; Yurchenco and Furthmayr, 1984; Siebold et al., 1987; Yurchenco and Ruben, 1987). The majority of the EMB-9 molecule consists of a central Gly-X-Y repeat domain, which forms a triple-helical structure. There are 17 sites at which the triple-helical structure is interrupted. In the *xd51* mutant, the conserved Gly at codon 258 is changed into Glu (Fig. 2*A*). Glycine is the only amino acid that can fit inside the triple helix, so this change presumably disrupts the assembly of the collagen trimer.

To test whether loss of *emb-9* function causes the formation of ectopic boutons, we examined other *emb-9* alleles. Complete loss of *emb-9* function leads to embryonic arrest. Thus, we examined the temperature-sensitive allele *b189* (Gupta et al., 1997). At the restrictive temperature (25°C), almost 100% of *b189* animals died at embryonic stages (Wood et al., 1980). At the subrestrictive temperature (22°C), some *b189* animals survived, and ~38% of surviving *b189* adults ($n = 128$) developed ectopic boutons. We

further created *emb-9* (*xd51/b189*) trans-heterozygote animals. At 22°C, these animals displayed a similar phenotype to *xd51* homozygotes (Fig. 2*B*). In addition, *xd51* trans-heterozygotes with the null allele *g23cg46* (*xd51/g23cg46*) showed a severe ectopic bouton defect like *xd51* homozygotes (Fig. 2*C*,*D*). Together, these data suggest that *xd51* may represent a strong loss-of-function allele in terms of the presynaptic defect. Increasing the *emb-9* level by overexpression did not lead to an ectopic bouton phenotype (data not shown). *emb-9* is expressed in body wall muscles, a subset of neurons, and other tissues (Graham et al., 1997). When we expressed *emb-9* in body wall muscle with the *Punc-54* promoter (Okkema et al., 1993), the presynaptic defect of *xd51* was significantly rescued ($n = 134$) (Fig. 2*D*). Neuronal expression in DD, VD, and AS neurons alone, driven by the *Phmr-1b* promoter (Broadbent and Pettitt, 2002), completely failed to rescue *xd51* ($n = 81$) (Fig. 2*D*). However, when coinjected with *Punc-54*::EMB-9, this neuronally expressed EMB-9 enhanced the rescue activity of muscle-derived *emb-9* (Fig. 2*D*). This implies that *emb-9* probably functions cell nonautonomously and that the muscle tissue may be the major source of the EMB-9 that is required for regulating presynapse growth.

let-2 encodes the sole Type IV collagen $\alpha 2$ chain (Guo et al., 1991; Sibley et al., 1993, 1994). We examined the presynaptic phenotype of *let-2* mutants as well. Because the null allele of *let-2* is also embryonic lethal, the temperature-sensitive mutant *let-2(g30)* was tested. At 20°C or above, almost all *let-2(g30)* animals are arrested at embryonic or larval stages (Sibley et al., 1994), thus preventing further phenotypic analysis. However, we noticed that, even at the permissive temperature (16°C), ~50% of *g30* animals ($n = 113$) display the ectopic bouton phenotype (Fig. 2*E*), indicating that the Type IV collagen $\alpha 2$ chain is also required for restricting presynaptic bouton growth.

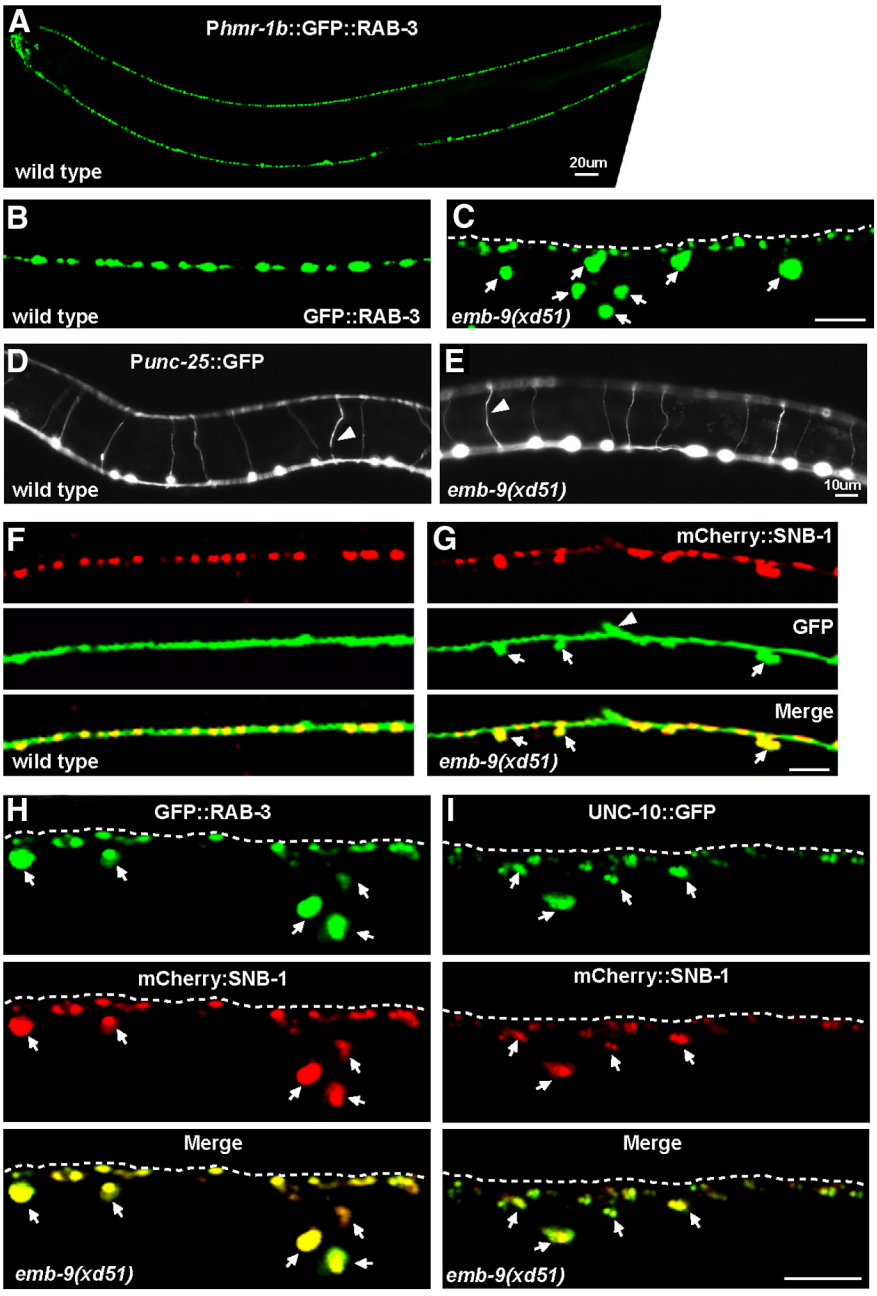

Figure 1. Ectopic boutons in *xd51* mutant animals. ***A***, Expression of the synaptic vesicle marker P*hmr-1b*::GFP::RAB-3 in *en passant* synapses in DD, VD, and AS motor neurons. Each GFP punctum may represent an individual presynaptic bouton. ***B***, P*hmr-1b*::GFP::RAB-3 puncta along the dorsal nerve cord in wild-type animals. ***C***, Ectopic GFP::RAB-3 puncta (arrows) appear in *emb-9(xd51)* mutant animals. Dashed line indicates the dorsal cord. ***D***, ***E***, P*unc-25*::GFP marker highlights the longitudinal and commissural processes of DD and VD neurons in wild-type and *emb-9(xd51)* animals. Triangles point to commissures. ***F***, ***G***, Double labeling with P*unc-25*::mCherry::SNB-1 and P*unc-25*::GFP, which marks neuronal processes in wild-type (***F***) and *xd51* mutant animals (***G***). Triangles represent the commissural junctions. ***H***, The synaptic vesicle marker P*hmr-1b*::GFP::RAB-3 (green) colocalizes with another synaptic vesicle marker P*hmr-1b*::mCherry::SNB-1 (red) on the ectopic boutons (arrows) in *emb-9(xd51)* mutants. ***I***, The active zone marker P*unc-25*::UNC-10::GFP (green) colocalizes with the synaptic vesicle marker P*unc-25*::mCherry::SNB-1 (red) on the ectopic boutons (arrows) in *emb-9(xd51)* mutants. Scale bars, 5 μm, unless otherwise labeled.

Collagen XVIII also functions in restricting presynaptic boutons

The major BM molecules identified in vertebrates have well-conserved orthologs in *C. elegans* (Hutter et al., 2000). To systematically investigate the role of BM in presynaptic bouton growth, we scanned the loss-of-function phenotypes of these BM orthologs using mutants and/or RNAi treatment (Kramer, 2005) (Table 1). In the RNAi-treated samples, we observed characteristic defects caused by loss of function of the genes, including *lam-3* (embryonic and larval lethal) (Huang et al., 2003), *lam-2* (embryonic lethal) (Huang et al., 2003), *ost-1* (clear, small worms) (Schwarzbauer and Spencer, 1993; Fitzgerald and Schwarzbauer, 1998), and *pat-2* (embryonic lethal) (Williams and Waterston, 1994), indicating that the RNAi treatments had indeed knocked down the corresponding genes (data not shown). *C. elegans* has two α laminins (LAM-3 and EPI-1), a single β laminin (LAM-1), and a single γ laminin (LAM-2) (Kramer, 2005). In *lam-3*, *epi-1*, or *lam-2* single loss-of-function mutants, no obvious presynaptic

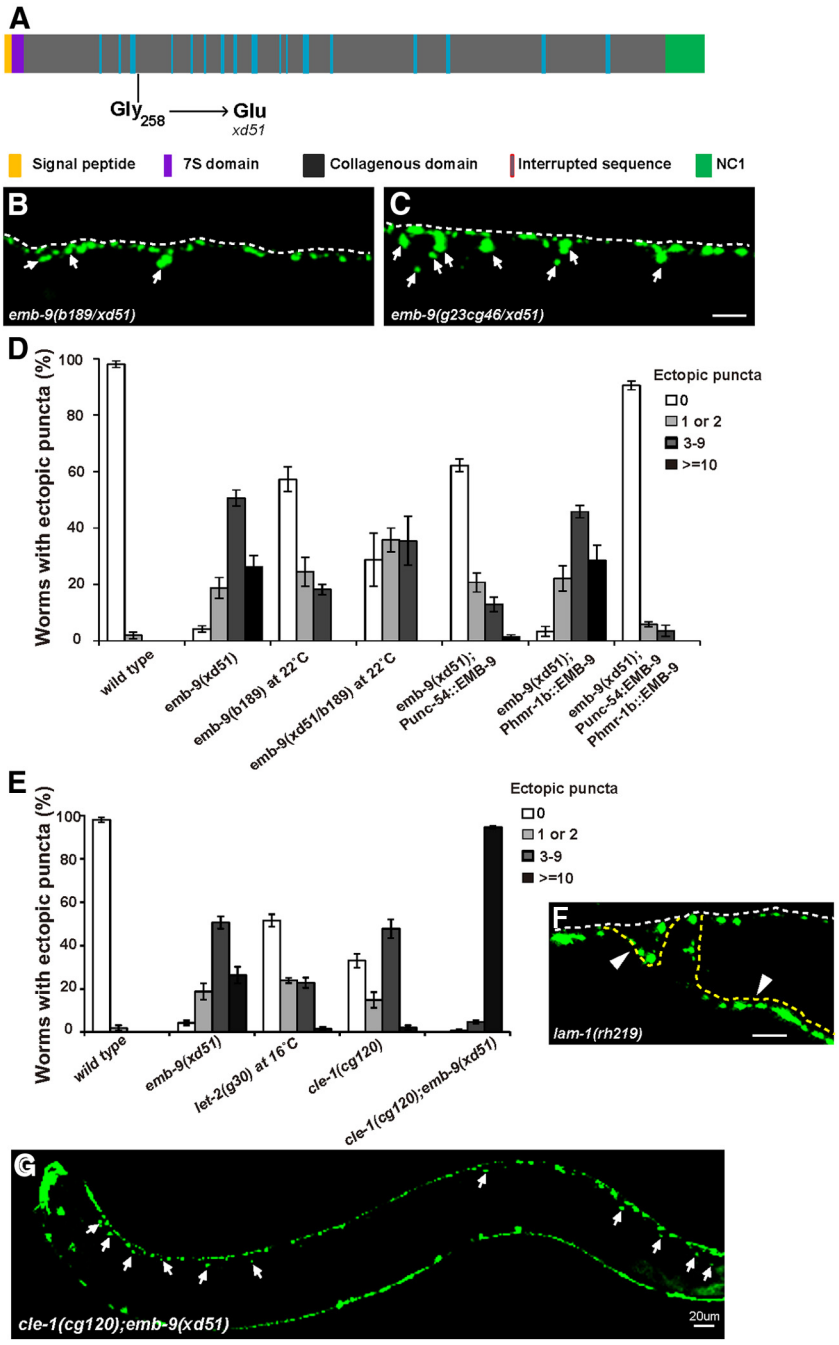

Figure 2. Loss of function of Type IV and XVIII collagen genes leads to the formation of ectopic presynaptic boutons. ***A***, Schematic representation of the EMB-9 protein (Type IV collagen α1 chain). The molecular lesion in *xd51* is indicated. ***B***, ***C***, Heterozygous *xd51/b189* and *xd51/cg46* mutants display the ectopic presynaptic bouton phenotype. White arrows indicate the ectopic boutons labeled by P*hmr-1b*::GFP::RAB-3. Scale bar, 5 μm. ***D***, Quantification of ectopic boutons using the P*hmr-1b*::GFP::RAB-3 marker in wild-type, *emb-9(xd51)*, *emb-9(b189)*, *emb-9(xd51/b189)*, and corresponding *emb-9* rescuing strains. The P*unc-54* and P*hmr-1b* promoters drive EMB-9 expression in muscle and neural tissue (DD, VD, and AS neurons), respectively. Young adult animals were scored. The columns represent the percentage of animals with 0, 1–2, 3–9, or $\geq$10 extra presynaptic boutons on the dorsal side. Error bars indicate the SEM. ***E***, Quantification of ectopic boutons using the P*hmr-1b*::GFP::RAB-3 marker in wild-type, *emb-9(xd51)*, *let-2(g30)*, *cle-1(cg120)*, and *cle-1(cg120);emb-9(xd51)* animals. ***F***, Irregular P*hmr-1b*::GFP::RAB-3 puncta appear on the misguided axons of *lam-1(rh219)* animals (yellow dashed lines). ***G***, P*hmr-1b*::GFP::RAB-3 puncta appear along the whole dorsal side in *cle-1(cg120);emb-9(xd51)* animals. Scale bars, 5 μm, unless otherwise labeled.

defect could be detected (Table 1). A total of 100% of *lam-1(rh219)* animals displayed fasciculation and axon guidance defects, and irregular RAB-3 puncta were observed on both normal and misguided axons (Fig. 2*F*). The abnormal axon tracts and synaptic morphology indicate that *lam-1* may play a pleiotropic role in both axon guidance and synapse development. We also tested the single *C. elegans* homologs of nidogen (NID-1) and perlecan (UNC-52) and found that loss of function of *nid-1* or *unc-52* did not cause any abnormality in restricting presynapse growth (Table 1). The protein encoded by *cle*-1 is closely related to vertebrate collagens Type XV and XVIII (Ackley et al., 2003). In the strong loss-of-function allele *cle-1(cg120)*, however, we found that ~60% of animals ($n = 118$) display ectopic RAB-3 puncta, suggesting that collagen Type XVIII is involved in presynapse restriction (Fig. 2*E*).

We found that both Type IV and XVIII collagens are involved in restricting presynapse growth. Therefore, double mutant analyses were performed to address the genetic interaction between these two. In *cle-1(cg120);emb-9(xd51)* double mutants, the abnormal presynaptic phenotype is dramatically enhanced (Fig. 2*G*). Of 145 animals examined, 94% display a strong presynaptic bouton overgrowth defect (Fig. 2*E*). As shown in Figure 2*G*, ectopic GFP::RAB-3 puncta display along the whole dorsal cord in *cle-1(cg120);emb-9(xd51)* animals. Thus, collagen IV and XVIII may function together to regulate presynapse restriction.

In the *cle-1(cg120);emb-9(xd51)* double mutants, we noticed that the number of GFP::RAB-3 puncta within the dorsal cord is significantly lower than in wild-type. A previous study also reported that *cle-1* display enlarged presynapses (Ackley et al., 2005). Therefore, the size and density of dorsal cord presynapses were measured (Fig. 3*A*,*B*). In *emb-9(xd51)* animals, the average size of GFP::RAB-3 puncta is $1.6 \pm 0.1\ \mu m^2$, which is similar to wild-type ($1.7 \pm 0.1\ \mu m^2$). Presynaptic size is significantly enlarged in *cle-1(cg120)* ($2.6 \pm 0.2\ \mu m^2$) ($p < 0.001$). Meanwhile, the presynaptic density in *cle-1(cg120)* (19.7 ± 1.9 puncta/100 μm) is considerably decreased compared with wild-type (30.0 ± 2.8 puncta/100 μm) ($p < 0.05$). In contrast, the presynaptic density of *emb-9(xd51)* (23.2 ± 1.0 puncta/100 μm) is similar to that of wild-type. In *cle-1(cg120);emb-9(xd51)* doubles, although the presynaptic size ($1.4 \pm 0.1\ \mu m^2$) is not significantly different from wild-type ($p > 0.05$), the presynaptic density is further decreased (15.4 ± 1.2 puncta/100 μm) compared with *cle-1(cg120)* single mutants (19.7 ± 1.9 puncta/100 μm) ($p < 0.05$). Thus, *emb-9* and *cle-1* may play roles in presynapse formation in addition to restricting presynaptic boutons.

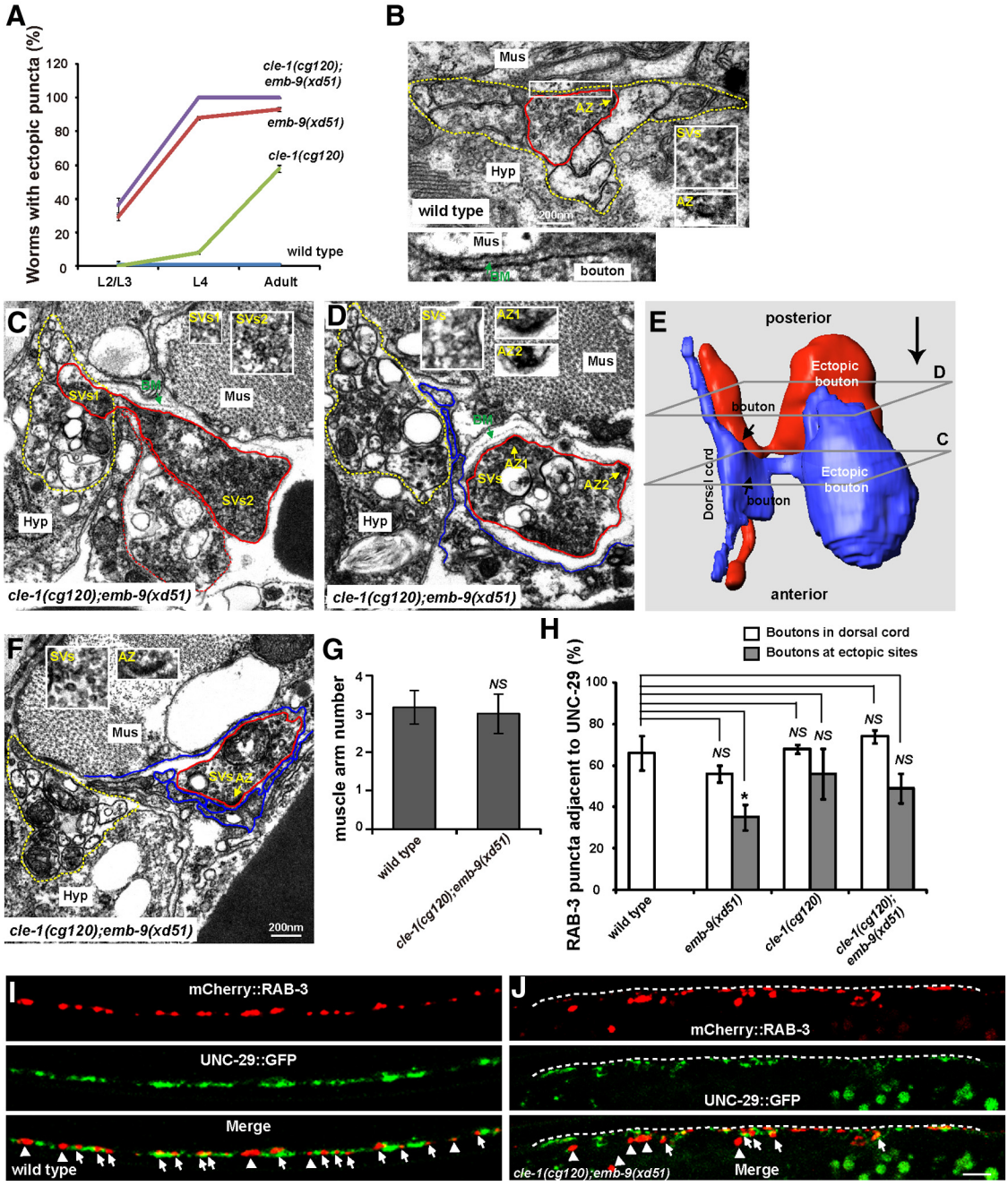

Figure 3. Ectopic boutons contain presynaptic structure. ***A***, Ectopic boutons gradually appear in *emb-9(xd51)*, *cle-1(cg120)*, and *cle-1(cg120);emb-9(xd51)* animals during development. ***B***, EM image of a typical presynaptic bouton (outlined with a red line) within the dorsal cord (outlined with dashed yellow lines) in wild-type. Insets, Cluster of synaptic vesicles (SVs) and electron-dense active zone region (AZ) characteristic of presynaptic boutons. Bottom, Enlargement of the boxed area to show the synaptic cleft, which contains the BM. Mus, Muscle; Hyp, hypodermal ridge. ***C***, An EM section showing an ectopic bouton (outside of dorsal cord) connected to an existing presynaptic bouton within the dorsal cord. A chased presynaptic bouton is outlined in red; the dorsal cord is outlined by the yellow dashed line. Dashed red line indicates another ectopic bouton, which is shown in blue in the 3D constructed image in ***E***. The ectopic bouton contains clusters of SVs1 and SVs2 (insets). ***D***, Two darkly stained AZs are present in a single ectopic bouton (AZ1 and AZ2, insets). Synaptic vesicle clusters are noticed in inset. ***E***, 3D reconstruction, using 65 serial EM sections, of two ectopic presynaptic boutons, which are connected with existing boutons within the dorsal cord. The cross-sections for images in ***C***, ***D*** are indicated. The orientation of the EM micrographs in ***C***, ***D*** is indicated by a large arrow on the upper right. ***F***, EM image showing an ectopic bouton with an AZ facing muscle extensions and an accumulation of SVs. ***G***, The number of muscle arms in *cle-1(cg120);emb-9(xd51)* animals is similar to that in wild-type. ***H***, Percentages of mCherry::RAB-3 puncta adjacent to UNC-29::GFP in dorsal cord or at the ectopic presynaptic sites. *$p < 0.05$. NS, Not significant. Data are mean ± SEM. ***I***, ***J***, Colabeling with P*hmr-1b*::mCherry::RAB-3 (red) and P*unc-29*::UNC-29::GFP (green). Arrows indicate mCherry::RAB-3 puncta adjacent to UNC-29::GFP. Arrowheads indicate mCherry::RAB-3 puncta not adjacent to UNC-29::GFP. Scale bars, 5 μm.

Ectopic boutons progressively emerge during development

We wondered during which developmental stage the ectopic boutons appear. Therefore, we followed presynapse growth in wild-type, *emb-9(xd51)*, *cle-1(cg120)*, and *emb-9(xd51);cle-1(cg120)*. At the larval 1 stage (L1), the presynaptic structures of DD neurons are located along the ventral cord; VD and AS neurons are not yet born. During this stage, ectopic presynaptic puncta could not be unambiguously detected. At the L2/L3 stage, ectopic GFP::RAB-3 puncta emerged from regions near the dorsal nerve cord in 29% of *emb-9(xd51)* ($n = 150$) and 38% of

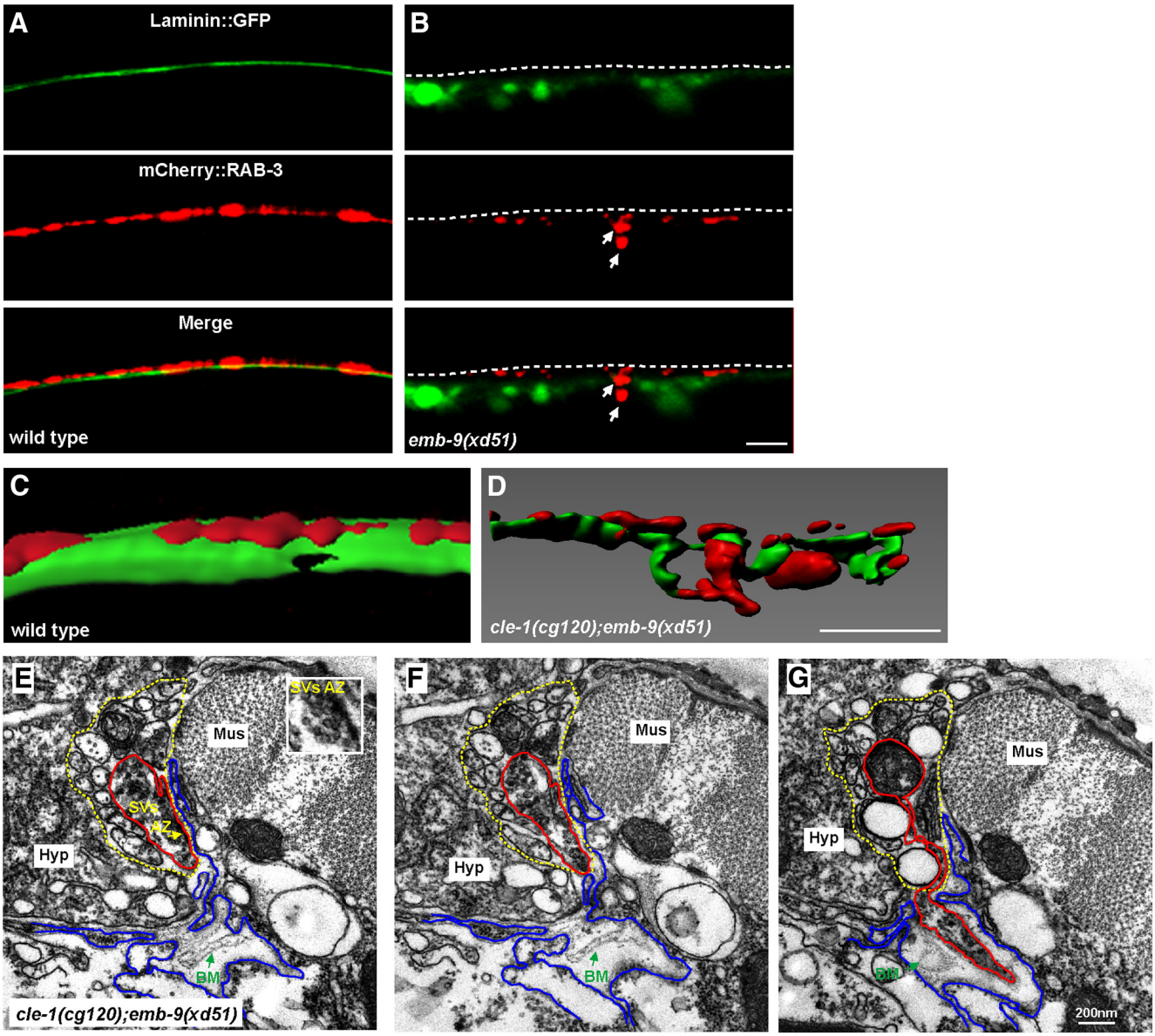

Figure 4. The integrity of the basement membrane is disrupted around the ectopic presynaptic sites. ***A***, In wild-type, the smooth laminin::GFP sheet (green) is evenly distributed underneath presynapses labeled by P*hmr-1b*::mCherry::RAB-3 (red). Dashed lines indicate the dorsal cord region. ***B***, Laminin::GFP is diffuse and fragmented in *emb-9(xd51)* animals (B′), and ectopic presynaptic boutons (indicated by arrows) are intermingled with Laminin::GFP. ***C***, ***D***, 3D reconstruction of Laminin::GFP and P*hmr-1b*::mCherry::RAB-3 in wild-type (***C***) and *cle-1(cg120);emb-9(xd51)* (***D***) animals. ***E***, ***F***, Two adjoining EM sections show where an ectopic presynaptic bouton is going to emerge from an existing presynaptic bouton (red lines) within the dorsal cord (yellow dashed lines). The loosely distributed BM (green arrows) is detached from muscle (blue lines) or neuron cells (red lines). Mus, Muscle; Hyp, hypodermal ridge. ***E***, Insets, Clusters of synaptic vesicles and a darkly stained active zone. ***G***, An ectopic bouton, originating from an existing presynapse, emerges from the dorsal cord (red line outlines synapses; yellow dashed line outlines dorsal cord). Scale bars, 5 μm.

emb-9(xd51);cle-1(cg120) ($n = 66$) animals but not obviously in *cle-1(cg120)* mutants ($n = 66$) (Fig. 3*C*). At the L4 stage, ectopic RAB-3 puncta appeared in 8% of *cle-1(cg120)* animals ($n = 159$) (Fig. 3*C*). These data suggest that the ectopic boutons emerge progressively during animal development.

Ectopic boutons originate from existing synapses

Next, we addressed from which region of the neuronal process ectopic boutons emerge. To do this, serial electron microscopy (EM) analyses were performed on *emb-9(xd51);cle-1(cg120)* young adult animals, and four ectopic boutons were reconstructed to trace their origins within the dorsal cord. In contrast to wild-type presynapses, which are always kept within the dorsal cord region (Fig. 3*B*), we found that ectopic boutons appear outside of the dorsal cord (Fig. 3*C–E*). In addition, EM chasing revealed that all four ectopic boutons emerge from an area of a neuronal process within the dorsal cord that contains a large number of clustered synaptic vesicles, similar to a typical chemical presynaptic bouton in wild-type (Fig. 3*C*; and data not shown). One particular set of images captured the moment at which an ectopic bouton was connected through a neck-like structure to an existing presynaptic bouton within the dorsal cord (Fig. 3*C*,*E*). Based upon all four reconstructions, we suspected that the ectopic presynaptic boutons may emerge from existing presynapses within the dorsal cord.

Are the ectopic boutons genuine synapses? We analyzed the ectopic boutons in more detail by EM. Through reconstruction, we found that the ectopic boutons in *emb-9(xd51);cle-1(cg120)*

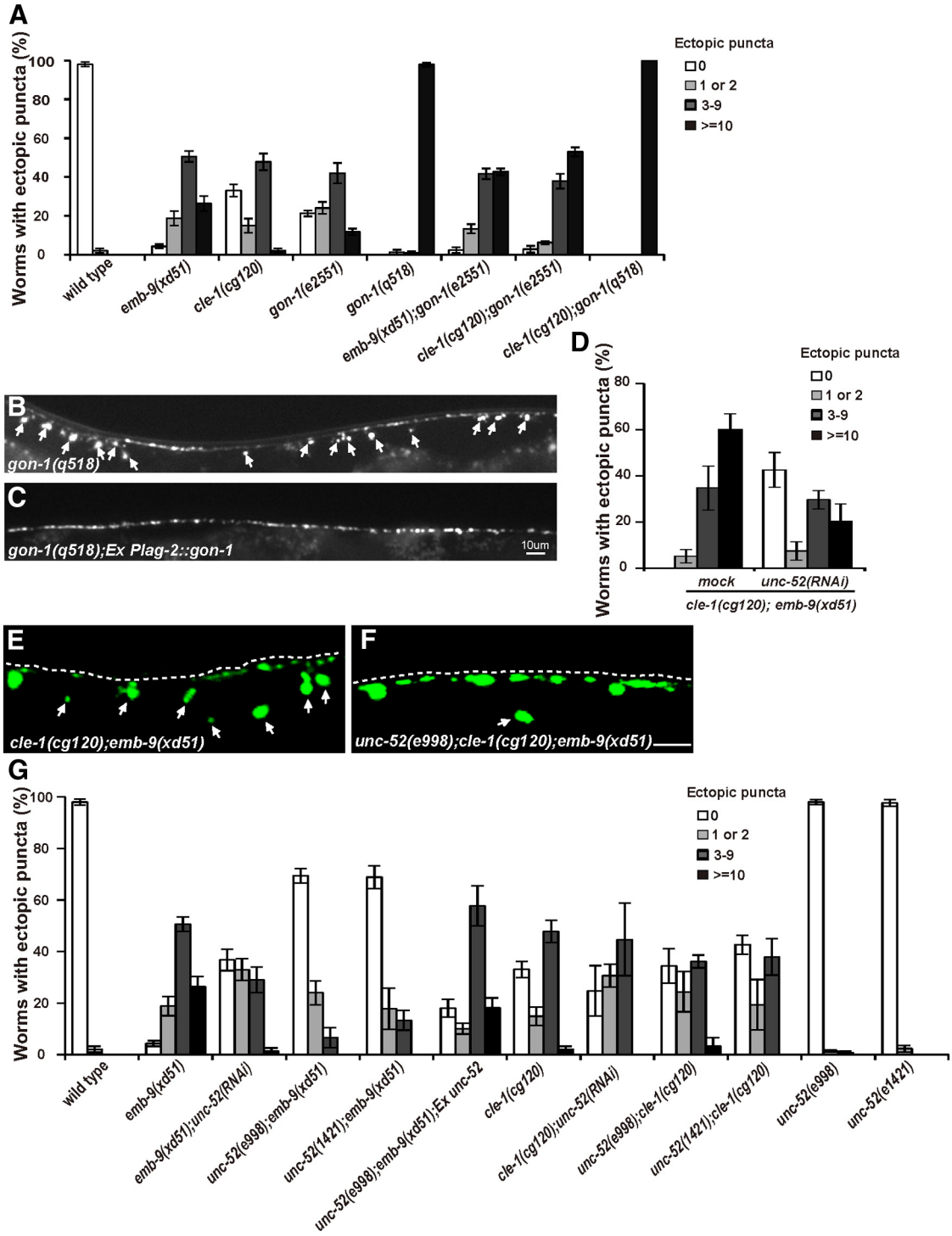

Figure 5. *unc-52* functions antagonistically to *emb-9*. ***A***, Quantification of ectopic boutons in the indicated basement membrane mutants. Young adult animals were scored. Error bars indicate the SEM. ***B***, *gon-1(q518)* mutants display strong synaptic defects with extra GFP::RAB-3 puncta along the whole dorsal side of the worm body (white arrows). ***C***, Expressing *gon-1* from distal tip cells using P*lag-2* promoter rescues the *gon-1* synaptic defect. ***D***, Quantification of ectopic P*hmr-1b*::GFP::RAB-3 puncta in *cle-1(cg120);emb-9(xd51)* double mutants treated with mock and *unc-52* RNAi. *unc-52* RNAi treatment significantly decreases the percentage of *cle-1(cg120);emb-9(xd51)* animals that display ectopic presynaptic boutons. ***E***, Ectopic P*hmr-1*b::GFP::RAB-3 puncta in *cle-1(cg120);emb-9(xd51)* (arrows). ***F***, The number of ectopic P*hmr-1b*::GFP::RAB-3 puncta (arrows) is lower in *unc-52(e998);cle-1(cg120);emb-9(xd51)* triple mutants. ***G***, Quantification of ectopic boutons for selected genotypes using the P*hmr-1b*::GFP::RAB-3 marker. The number of ectopic boutons is lower in *emb-9(xd51);unc-52(RNAi)*, *unc-52(e998);emb-9(xd51)*, and *unc-52(e1421);emb-9(xd51)* animals compared with *emb-9(xd51)*. Scale bars, 5 μm.

animals possess the characteristic features of presynapses, including accumulation of synaptic vesicles and darkly stained active zones (Fig. 3*D*,*F*), suggesting that the ectopic boutons may contain properly assembled presynaptic structures. Interestingly, we noticed that three of four ectopic boutons contained more than two active zones (Fig. 3*D*). We also examined presynapses within the dorsal cord in *emb-9(xd51);cle-1(cg120)* animals and found that each presynapse tends to contain only one active zone (n = 10). In addition, the average size of the four ectopic boutons (1.21 ± 0.12 μm in diameter) appears larger than that of presyn-

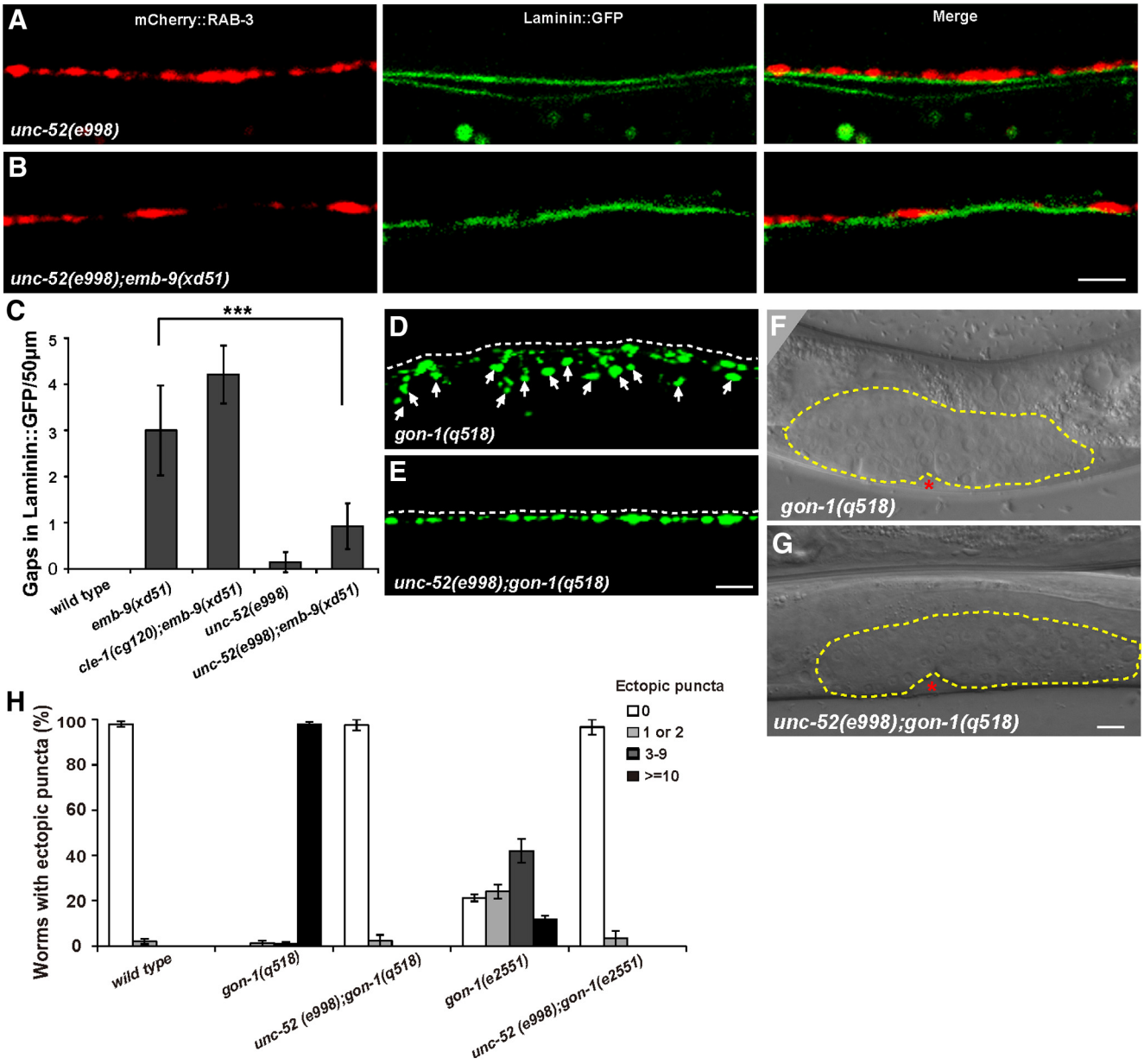

Figure 6. BM integrity is improved by *unc-52* mutation. ***A***, Double labeling with P*hmr-1b*::mCherry::RAB-3 (red) and Laminin::GFP (green) in *unc-52(e998)* mutants. ***B***, Double labeling with P*hmr-1b*::mCherry::RAB-3 (red) and Laminin::GFP (green) in *unc-52(e998);emb-9(xd51)* animals. ***A***, ***B***, The P*hmr-1b*::mCherry::RAB-3 puncta tightly align with Laminin::GFP. ***C***, Quantification of BM integrity based on the number of gaps per 50 μm length of Laminin::GFP. ***$p < 0.001$. ***D***, Ectopic synaptic boutons labeled by P*hmr-1b*::GFP::RAB-3 (arrows) in *gon-1(q518)* animals. ***E***, The ectopic presynaptic bouton defect is greatly suppressed in *unc-52(e998);gon-1(q518)* mutants compared with *gon-1(q518)*. ***F***, ***G***, The gonad arm underextension defect in *gon-1(q518)* mutants is not suppressed in *unc-52(e998);gon-1(q518)* animals. Dashed lines highlight the gonad regions. ***H***, Quantification of ectopic boutons for selected genotypes using the P*hmr-1b*::GFP::RAB-3 marker. The number of ectopic boutons is significantly lower when *gon-1* is doubled with *unc-52(e998)*. Scale bars, 5 μm.

apses in the dorsal cord (0.40 ± 0.08 μm in diameter) in *emb-9(xd51);cle-1(cg120)* double mutants. However, we should point out that the ectopic boutons that are more easily traced under EM tend to be the large ones. It is not appropriate at this moment to conclude that ectopic boutons are indeed larger than regular synapses within the dorsal cord. In contrast, the average size of dorsal cord presynapses in wild-type animals (0.42 ± 0.03 μm in diameter, $n = 5$) is similar to that in *emb-9(xd51);cle-1(cg120)* mutants ($p > 0.05$). This observation agrees well with the measurements using the GFP::RAB-3 marker.

Ectopic boutons may target muscles

Based on EM images, we noticed that the ectopic presynaptic boutons are surrounded by muscle cell extensions (Fig. 3*C*,*D*,*F*, blue lines), namely, muscle arms in worms. Noticeably, some active zones within ectopic boutons are apposed to muscle arms, with thin basement membrane between (Fig. 3*F*). Some active zones face muscles but are kept apart from the muscle by multiple layers of loosely connected basement membrane (Fig. 3*D*). Because visible postsynaptic specializations are generally lacking in worms (White et al., 1986), we addressed whether the ectopic boutons could target muscle cells by performing the following experiments.

First, we examined the muscle cell extensions using fluorescence markers. P*him-4*::Mb::YFP labels distal muscle cells, allowing extended muscle arms to be visualized (Dixon and Roy, 2005). Thus, we introduced this P*him-4*::Mb::YFP marker into wild-type and *emb-9(xd51);cle-1(cg120)* double mutants. Quan-

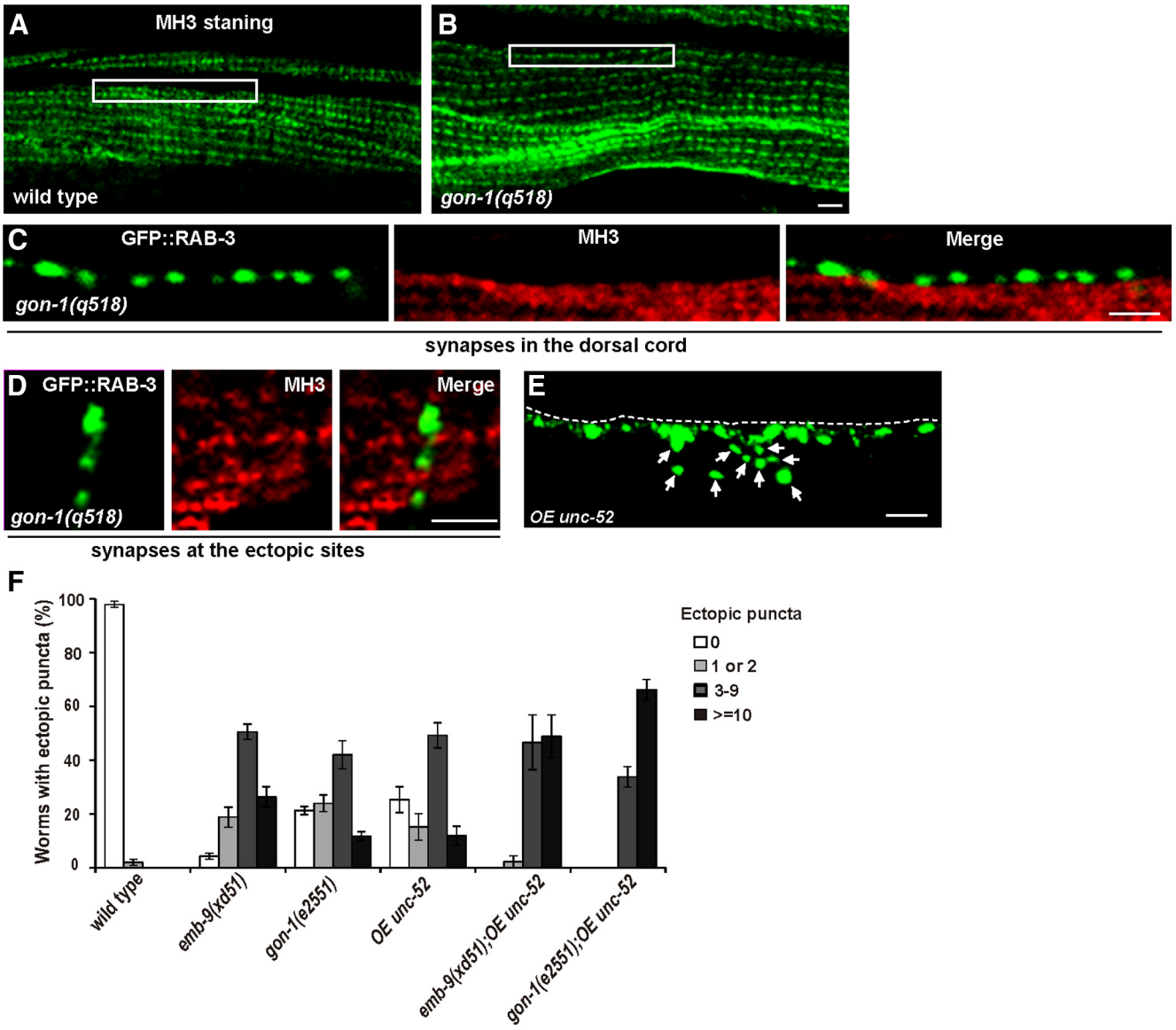

Figure 7. *unc-52* promotes ectopic presynaptic bouton growth. MH3 stains UNC-52 protein on body wall muscle in wild-type animals (***B***) and *gon-1(q518)* mutants (***A***). White boxes indicate the edge of the dorsal left muscle quadrant, which is the putative neuromuscular region along the dorsal cord. ***C***, Double labeling of the dorsal cord region in *gon-1(q518)* mutants with P*hmr-1b*::GFP::RAB-3 (green) and MH3 staining (red). ***D***, Double labeling of the ectopic presynaptic region in *gon-1(q518)* mutants with P*hmr-1b*::GFP::RAB-3 (green, ***D′***) and MH3 staining (red, ***D′′***). ***E***, Overexpression of *unc-52* leads to the formation of ectopic boutons labeled by P*hmr-1b*::GFP::RAB-3 (arrows). ***F***, Quantification of the ectopic bouton defect in selected genotypes. The ectopic presynaptic bouton defect in *emb-9(xd51)* or *gon-1(e2551)* animals is enhanced by *unc-52* overexpression. Error bars indicate the SEM. Scale bars, 5 μm.

tification of muscle arm number from the same muscle on the dorsal side (D.R 11) showed that both wild-type and *emb-9(xd51);cle-1(cg120)* double mutants extended a similar number of muscle arms to contact the dorsal cord (Fig. 3*G*), suggesting that the muscle extension is not affected in *emb-9(xd51);cle-1(cg120)* double mutants.

Second, we asked whether the ectopic boutons codistribute with postsynaptic components. UNC-29 is the acetylcholine receptor on body muscle cells (Fleming et al., 1997). With the functional P*unc-29*::UNC-29::GFP marker (Fleming et al., 1997), the acetylcholine receptor clusters on all muscle cells could be visualized. Meanwhile, on the dorsal cord, the P*hmr-1b*::mCherry::RAB-3 marker labels the presynaptic structures only in DD GABA and AS acetylcholine neurons. Therefore, in wild-type animals, ~67% of mCherry::RAB-3 puncta are adjacent to UNC-29::GFP signal, suggesting that these RAB-3 dots may represent acetylcholine synapses (Fig. 3*H*,*I*). This juxtaposition is not drastically changed along the dorsal cord in *emb-9(xd51)*, *cle-1(cg120)*, or *cle-1(cg120);emb-9(xd51)* animals (Fig. 3*H*,*J*). At the ectopic bouton sites, a significant proportion of RAB-3::mCherry puncta are still juxtaposed with UNC-29::GFP (49%), suggesting that some of these ectopic boutons may target muscle cells through the corresponding postsynaptic receptors (Fig. 3*H*,*J*).

BM integrity is disrupted at the ectopic bouton sites

Both Type IV and XVIII collagens are key components of the BM. We wondered whether the BM integrity is affected in mutants with ectopic boutons. Therefore, we examined the BM morphology using the P*lam-1*::Laminin::GFP marker (Ihara et al., 2011). In wild-type animals, laminin (Laminin::GFP) forms a smooth sheet-like structure underlying RAB-3 puncta (Fig. 4*A*). In *emb-9(xd51)* mutants, the tight association between laminin and RAB-3 is disrupted (Fig. 4*B*). In the region where ectopic RAB-3

puncta appear, the laminin::GFP signal tends to be fragmented (Fig. 4*B*, arrows). *cle-1(cg120);emb-9(xd51)* mutants display a severe ectopic bouton phenotype (Fig. 2*E*,*G*). As shown with 3D reconstructions, whereas presynapses are restricted to a distinct BM boundary in wild-type animals (Fig. 4*C*), the ectopic boutons are intermingled with Laminin::GFP in *cle-1(cg120);emb-9(xd51)* animals (Fig. 4*D*). In addition, various breaks in the Laminin::GFP sheet were observed in the region where the ectopic boutons emerge (Fig. 4*D*). The BM morphology in *cle-1(cg120);emb-9(xd51)* was further examined under EM. Deformed BM, sometimes with multiple folds, was detected between the dorsal cord and the muscle before (Fig. 4*E*,*F*) and after (Fig. 4*G*) ectopic synapses emerged. In contrast, BM was detected as a thin single-layer electron-dense structure closely adjacent to the synaptic region in wild-type animals (Fig. 3*B*) or *cle-1(cg120);emb-9(xd51)* mutants in dorsal cord regions where no ectopic boutons were emerging. This suggests that the deformed BM structure surrounding the ectopic bouton region is unlikely to result from an EM fixation artifact, and is instead a consequence of the formation of ectopic boutons.

ADAMTS9/GON-1 functions similarly to collagen IV and XVIII

Modulation of BM is mediated by matrix metalloproteinases, a group of zinc-dependent proteases that regulates extracellular matrix composition, organization, and function through cleavage of matrix components (Vu and Werb, 2000). Previous reports showed that the ADAMTS family members GON-1/ADAMTS and MIG-17/ADAMTS function together with BM components (Hesselson et al., 2004; Kubota et al., 2004). A recent study also showed that a putative gain-of-function allele of *emb-9* can suppress the gonad migration defect caused by loss of *gon-1* function (Kubota et al., 2012). Interestingly, loss of function of *gon-1* causes ectopic boutons, similar to *emb-9* and *cle-1* mutants (Fig. 5*A*,*B*). In the null allele *gon-1(q518)*, >40 ectopic GFP::RAB-3 dots distribute along the periphery of the whole dorsal cord in almost all young adults tested (Fig. 5*A*,*B*). In contrast, loss of function of other ADAMTS genes (*mig-17*, *unc-71*, *adt-1*, or *sup-17*) did not lead to any obvious ectopic boutons (Table 1).

To test the putative genetic interactions between *gon-1* and *emb-9* or *cle-1*, we made the double mutants *cle-1(cg120);gon-1(e2551)* and *emb-9(xd51);gon-1(e2551)*. In these double mutants, the ectopic bouton phenotype is enhanced in comparison with *cle-1(cg120)*, *emb-9(xd51)*, or *gon-1(e2551)* single mutants (Fig. 5*A*). We further created *cle-1(cg120);gon-1(q515)* double mutants and found that the ectopic presynaptic defect is indistinguishable from *gon-1(q518)* single mutants (Fig. 5*A*). Although the strong lethality of *emb-9(xd51);gon-1(q518)* animals prevents further analysis, the above data suggest that *gon-1* may function in the same pathway as *emb-9* and *cle-1*. A previous study demonstrated that *gon-1* is required for gonad distal tip cell migration. When *gon-1* was expressed in the gonad distal tip cell using the P*lag-2* promoter (Henderson et al., 1994), ectopic presynaptic growth was significantly rescued (Fig. 5*B*,*C*), suggesting that *gon-1* may function cell nonautonomously.

unc-52 functions antagonistically to *emb-9*

Type IV and XVIII collagens are required for restricting presynaptic growth, and *cle-1(cg120);emb-9(xd51)* animals display a strong ectopic bouton defect. We wondered whether there are BM components that play negative roles in presynapse restriction. Therefore, dsRNAs corresponding to individual major BM components were injected into *cle-1(cg120);emb-9(xd51)* animals, and genetic suppressors were identified based on alleviation of the ectopic bouton phenotype. From the screen, we found that *unc-52* RNAi treatment significantly rescued the ectopic presynaptic defect in *cle-1(cg120);emb-9(xd51)* animals (Fig. 5*D*) ($p < 0.0001$).

unc-52 encodes the *C. elegans* ortholog of mammalian perlecan (Rogalski et al., 1993). Full loss of *unc-52* function causes severe defects in myofilament lattice assembly in body wall muscle and finally leads to embryonic arrest (Hresko et al., 1994). In *unc-52(e998)* or *unc-52(e1421)* partial loss-of-function mutants, no ectopic boutons could be detected (Table 1; Fig. 5*G*). To examine whether the *unc-52* mutant could suppress the *cle-1(cg120);emb-9(xd51)* phenotype, we constructed the *unc-52(e998);cle-1(cg120);emb-9(xd51)* triple mutant. We found that the strong ectopic bouton phenotype of *cle-1(cg120);emb-9(xd51)* was substantially suppressed by *unc-52(e998)* (Fig. 5*E*,*F*). To reveal which mutation is suppressed by *unc-52*, *unc-52* RNAi treatment was performed in *emb-9(xd51)* and *cle-1(cg120)* animals. We found that only the *emb-9* mutant phenotype was suppressed by *unc-52* RNAi. In addition, we constructed *unc-52(e998);emb-9(xd51)*, *unc-52(e1421);emb-9(xd51)*, *cle-1(cg120);unc-52(e1421)*, and *cle-1(cg120);unc-52(e998)* double mutants. Based on phenotypic analysis, we again found that only the ectopic bouton phenotype in *emb-9* mutants could be suppressed by *unc-52* mutation (Fig. 5*G*). Thus, *unc-52* functions antagonistically to *emb-9* but not to *cle-1*. To further test whether the suppression is due to loss of function of *unc-52*, we introduced a wild-type copy of *unc-52* into *unc-52(e1421);emb-9(xd51)* animals and found that the genetic suppression was significantly alleviated (Fig. 5*G*). Thus, the suppression on *emb-9* is indeed caused by loss of function of the *unc-52* gene.

We further tested whether the BM defect in *emb-9* mutants could be suppressed by *unc-52*. In *unc-52(e998)* animals, the laminin::GFP is mostly intact and RAB-3 puncta are closely associated with laminin, which mimics the wild-type phenotype (Figs. 4*A* and 6*A*). Compared with the fragmented laminin structure in *emb-9(xd51)* single mutants (Fig. 4*B*), the laminin::GFP is more evenly distributed and tightly coupled with mCherry::RAB-3 puncta in *unc-52(e998);emb-9(xd51)* double mutants (Fig. 6*B*), suggesting that the BM integrity is probably improved. In addition, the BM fragmentation in *emb-9(xd51)* is also alleviated in *unc-52(e998);emb-9(xd51)* (Fig. 6*C*), suggesting that the BM integrity is improved by *unc-52*.

unc-52 promotes ectopic bouton growth

emb-9 mutants display a similar phenotype to *gon-1* animals. We wondered whether loss of *unc-52* function could also suppress *gon-1*. In *unc-52(e998);gon-1(q518)* mutants, we found that the ectopic presynapse phenotype was dramatically suppressed compared with *gon-1(q518)* single mutants (Fig. 6*D*,*E*). We further created *unc-52(e998); gon-1(e2551)* and found that the ectopic bouton phenotype associated with the *e2551* allele could also be suppressed by *unc-52* mutation (Fig. 6*H*). Interestingly, the suppression is restricted to the presynaptic phenotype; the gonad extension defect of *gon-1* is not suppressed (Fig. 6*F*,*G*).

ADAMTS family proteases degrade BM proteoglycans, such as aggrecan and versican (Somerville et al., 2003). Could perlecan/UNC-52 serve as the enzymatic substrate of GON-1? If so, we would expect that the UNC-52 expression level should be increased in *gon-1*-defective animals. The MH3 antibody recognizes the UNC-52 isoforms produced by body wall muscle cells (Francis and Waterston, 1991; Hresko et al., 1994; Mullen et al., 1999). Staining with MH3 showed that the expression pattern

and level of muscle UNC-52 in *gon-1* mutant animals is indistinguishable from wild-type (Fig. 7*A*,*B*). At the putative NMJ region on the dorsal cord (boxed region in Fig. 7*A*,*B*), similar levels of MH3 staining signal could be observed. These data suggest that GON-1 cannot degrade muscle UNC-52, or alternatively that the putative cleaved product of UNC-52 still retains the antigen recognized by MH3. We further analyzed the relationship between synapses and UNC-52 protein localization in *gon-1* mutants. In the dorsal cord region, RAB-3::GFP puncta localize next to UNC-52 (Fig. 7*C*). At the ectopic bouton region, the RAB-3::GFP puncta also localize adjacent to UNC-52 (Fig. 7*D*), suggesting that *gon-1* does not influence the relative position of presynapses and UNC-52.

Perlecan/UNC-52 plays an opposing role to both Type IV collagen (EMB-9) and ADAMTS/GON-1, suggesting that UNC-52 may be a major negative regulator in restricting presynapse growth. Therefore, we tested whether increasing the UNC-52 level could promote untamed bouton formation. We introduced fosmid WRM0627aA11, which contains the entire *unc-52* gene locus, into wild-type animals, and found that it induced the formation of ectopic boutons, similar to those observed in *emb-9*, *cle-1*, or *gon-1* loss-of-function mutants (Fig. 7*E*,*F*). In fosmid WRM069dE06, the majority of the *unc-52* gene is removed, whereas some other genes overlapping with WRM0627aA11 remain intact. Overexpression of WRM069dE06 did not result in any obvious extra boutons (data not shown). Furthermore, increasing *unc-52* expression by injecting fosmid WRM0627Aa11 enhanced both the *emb-9(xd51)* and *gon-1(e2551)* mutant phenotypes (Fig. 7*F*) ($p < 0.001$). Together, these data indicate that UNC-52 promotes ectopic presynapse growth.

Discussion

In this study, we showed that the growth restriction of presynaptic boutons is regulated by complex interactions among different BM components. If the BM malfunctions, as in *emb-9*, *cle-1*, or *gon-1* mutants, ectopic boutons invade into nonsynaptic regions. Our work raises many intriguing questions.

The biological features of the ectopic boutons are particularly intriguing. Are they real synapses? Are they normal synapses? Are they functional? At present, we can only provide partial answers. The accumulation of vesicles and the darkly stained active zones visible under EM suggest that these ectopic boutons contain assembled presynaptic structures. However, the unusually large size and the presence of multiple active zones indicate that the ectopic boutons are not completely normal. Interestingly, these abnormalities do not extend to the presynapses within the dorsal cord in the same worm. Presynapses within the dorsal cord are much smaller and contain only one active zone, thus resembling regular presynapses in wild-type. One explanation for this phenomenon could be that the unknown signal that triggers presynapse growth at ectopic sites could also promote presynaptic overgrowth, for instance, by producing more synaptic vesicles and active zones. But why this overgrowth promotion only occurs on the ectopic boutons remains a mystery. The ectopic presynapses are clearly surrounded by muscle extensions. The relatively intact juxtaposition of RAB-3 with UNC-29 suggests that some ectopic presynapses could associate normal postsynaptic receptor clusters and thus may be functional. Because of technical limitations, single synapse recording cannot be performed in worms at present. With advanced electrophysiology, we may ultimately determine whether the ectopic synapses are functional or not.

Why do ectopic boutons originate from existing presynapses but not other nonsynaptic regions within the nerve cord? Many studies of both vertebrate and invertebrate NMJs indicate that the synaptic BM has a distinct molecular composition compared with BM surrounding the remainder of the myofiber (Ackley et al., 2001, 2003; Singhal and Martin, 2011). Thus, one possibility is that some differentially distributed molecules in the synaptic BM may send permissive signals to ectopic presynapses, allowing them to pass through, but only from the synaptic BM border. Alternatively, presynapses themselves may contain some special features, for instance, differently arranged cytoskeleton, which allow them (but not nonsynaptic regions) to break through the BM more easily. These speculations imply that the signal sensing the BM alteration may reside on or near the synapses. If this is the case, what is the sensor? Integrins (INA-1/PAT-2/PAT-3), dystroglycans (DGN-1/DGN-2/DGN-3), glypican (GPN-1/LON-2), and syndecan (SDN-1) could function as BM receptors to facilitate BM anchoring and signaling. However, scanning of loss-of-function mutations in single genes failed to identify any BM receptors that may play roles in presynaptic bouton restriction. Previous studies showed that both perlecan and collagen Type IV interact with integrin (Francis and Waterston, 1991; Gettner et al., 1995). We have now shown that *unc-52* and *emb-9* play opposing roles in presynapse restriction. Therefore, the failure to detect a role for integrin in restricting presynapse growth could be due to the simultaneous removal of both positive (collagen IV) and negative (perlecan) forces from the BM in integrin mutants. Alternatively, other BM receptors on synapses may fulfill the role of sensing changes in BM composition. Identification of the BM sensors on synapses or neurons will certainly greatly facilitate our understanding of the signal transduction pathway between neurons and their surrounding environment.

Another question is whether and how the development of ectopic presynapses is linked to the development of correctly positioned presynapses. We noticed that the presynaptic density along the dorsal cord is greatly decreased in *cle-1;emb-9* double mutants. Could there be a homeostatic balance between synapses at ectopic sites and those at proper locations? What is the regulator that controls synaptic homeostasis? A previous study hinted that some regulators may exist to define optimal regions along the nerve process for forming evenly distributed presynaptic structures while also preventing formation of fused, abnormally large presynapses (Zhen et al., 2000). It is not clear how this growth homeostasis among nerve cord presynapses is related to that between ectopic presynapses and presynapses at proper locations. Our current study certainly offers many opportunities for future investigations.

How does perlecan antagonize collagen IV and GON-1? It has been reported that collagen IV is required for incorporating perlecan into the BM of fly larvae (Pastor-Pareja and Xu, 2011). However, in mice homozygous for a targeted deletion of the collagen IV $\alpha1/\alpha2$ pair, the deposition of other BM components is not affected (Pöschl et al., 2004). Here, we simultaneously removed both collagen IV and perlecan using a genetic approach and found that the synaptic defect caused by loss of collagen IV function was dramatically suppressed by perlecan mutation. At present, it is difficult to pinpoint the exact molecular mechanism of this genetic suppression. However, we would like to hypothesize that, through multiple molecular interactions, perlecan keeps the collagen IV trimers apart. When collagen IV molecules are lost, the BM integrity is reduced. Further depleting perlecan, however, removes the instability created by *emb-9* mutation. Therefore, the remaining BM components collapse together and

reform a "functional" BM, thus keeping the presynapse at bay. Similar speculation could be made about the antagonistic role of perlecan on GON-1. However, detailed biophysical, biochemical, and *in vitro* reconstruction studies will be needed to clarify the complicated and intriguing role of multiple BM components in controlling synapse growth.

A number of independent genetic screens using fluorescently labeled presynaptic markers have identified a set of genes involved in synapse development in worms (Jin, 2002), and many of their vertebrate homologs have been implicated in CNS development or/and function (Wyszynski et al., 2002; Bloom et al., 2007; Wentzel et al., 2013). However, the molecular apparatus that restricts worm *en passant* synapses to their proper location has previously been poorly elucidated. We offer several explanations for this slow progress. Genes that regulate synapse restriction may be essential for animal development. For instance, both collagen Type IV α1 and α2 chains (EMB-9 and LET-2) are required for viability. Thus, their roles in synaptic development could be overlooked in genetic screens of healthy adults. Second, functional redundancy may mask the mutant phenotype resulting from a single gene mutation. Loss of function of *emb-9* or *cle-1* alone causes relatively subtle ectopic bouton defects, but *cle-1;emb-9* doubles display a much stronger phenotype. Third, markers labeling presynapses within a subset of neurons may be visually too weak to reveal ectopic boutons. Mutants with fewer ectopic presynapses (e.g., *emb-9* or *cle-1* single mutants) may be more easily spotted with markers that highlight more presynapses. With only 1800 genomes, our screen is far from saturation. In the future, more large-scale conditional and modifier screens could be performed. We are confident that the simple, elegant worm nervous system will continue to provide insights to improve fundamental understanding of nervous system development in higher organisms.

References

Ackley BD, Crew JR, Elamaa H, Pihlajaniemi T, Kuo CJ, Kramer JM (2001) The NC1/endostatin domain of *Caenorhabditis elegans* type XVIII collagen affects cell migration and axon guidance. J Cell Biol 152:1219–1232. CrossRef Medline

Ackley BD, Kang SH, Crew JR, Suh C, Jin Y, Kramer JM (2003) The basement membrane components nidogen and type XVIII collagen regulate organization of neuromuscular junctions in *Caenorhabditis elegans*. J Neurosci 23:3577–3587. Medline

Ackley BD, Harrington RJ, Hudson ML, Williams L, Kenyon CJ, Chisholm AD, Jin Y (2005) The two isoforms of the *Caenorhabditis elegans* leukocyte-common antigen related receptor tyrosine phosphatase PTP-3 function independently in axon guidance and synapse formation. J Neurosci 25:7517–7528. CrossRef Medline

Allamand V, Sunada Y, Salih MA, Straub V, Ozo CO, Al-Turaiki MH, Akbar M, Kolo T, Colognato H, Zhang X, Sorokin LM, Yurchenco PD, Tryggvason K, Campbell KP (1997) Mild congenital muscular dystrophy in two patients with an internally deleted laminin alpha2-chain. Hum Mol Genet 6:747–752. CrossRef Medline

Bloom AJ, Miller BR, Sanes JR, DiAntonio A (2007) The requirement for Phr1 in CNS axon tract formation reveals the corticostriatal boundary as a choice point for cortical axons. Genes Dev 21:2593–2606. CrossRef Medline

Brenner S (1974) The genetics of *Caenorhabditis elegans*. Genetics 77:71–94. Medline

Broadbent ID, Pettitt J (2002) The *C. elegans* hmr-1 gene can encode a neuronal classic cadherin involved in the regulation of axon fasciculation. Curr Biol 12:59–63. CrossRef Medline

Burns ME, Augustine GJ (1995) Synaptic structure and function: dynamic organization yields architectural precision. Cell 83:187–194. CrossRef Medline

Campanelli JT, Ferns M, Hoch W, Rupp F, von Zastrow M, Hall Z, Scheller RH (1992) Agrin: a synaptic basal lamina protein that regulates development of the neuromuscular junction. Cold Spring Harbor Symp Quant Biol 57:461–472. CrossRef Medline

Dixon SJ, Roy PJ (2005) Muscle arm development in *Caenorhabditis elegans*. Development 132:3079–3092. CrossRef Medline

Fischer von Mollard G, Mignery GA, Baumert M, Perin MS, Hanson TJ, Burger PM, Jahn R, Südhof TC (1990) rab3 is a small GTP-binding protein exclusively localized to synaptic vesicles. Proc Natl Acad Sci U S A 87:1988–1992. CrossRef Medline

Fitzgerald MC, Schwarzbauer JE (1998) Importance of the basement membrane protein SPARC for viability and fertility in *Caenorhabditis elegans*. Curr Biol 8:1285–1288. CrossRef Medline

Fleming JT, Squire MD, Barnes TM, Tornoe C, Matsuda K, Ahnn J, Fire A, Sulston JE, Barnard EA, Sattelle DB, Lewis JA (1997) *Caenorhabditis elegans* levamisole resistance genes lev-1, unc-29, and unc-38 encode functional nicotinic acetylcholine receptor subunits. J Neurosci 17:5843–5857. Medline

Fox MA, Sanes JR, Borza DB, Eswarakumar VP, Fässler R, Hudson BG, John SW, Ninomiya Y, Pedchenko V, Pfaff SL, Rheault MN, Sado Y, Segal Y, Werle MJ, Umemori H (2007) Distinct target-derived signals organize formation, maturation, and maintenance of motor nerve terminals. Cell 129:179–193. CrossRef Medline

Francis R, Waterston RH (1991) Muscle cell attachment in *Caenorhabditis elegans*. J Cell Biol 114:465–479. CrossRef Medline

Gesemann M, Denzer AJ, Ruegg MA (1995) Acetylcholine receptor-aggregating activity of agrin isoforms and mapping of the active site. J Cell Biol 128:625–636. CrossRef Medline

Gettner SN, Kenyon C, Reichardt LF (1995) Characterization of beta pat-3 heterodimers, a family of essential integrin receptors in *C. elegans*. J Cell Biol 129:1127–1141. CrossRef Medline

Graham PL, Johnson JJ, Wang S, Sibley MH, Gupta MC, Kramer JM (1997) Type IV collagen is detectable in most, but not all, basement membranes of *Caenorhabditis elegans* and assembles on tissues that do not express it. J Cell Biol 137:1171–1183. CrossRef Medline

Gray EG (1959) Axo-somatic and axo-dendritic synapses of the cerebral cortex: an electron microscope study. J Anat 93:420–433. Medline

Guo XD, Johnson JJ, Kramer JM (1991) Embryonic lethality caused by mutations in basement membrane collagen of *C. elegans*. Nature 349:707–709. CrossRef Medline

Gupta MC, Graham PL, Kramer JM (1997) Characterization of alpha1(IV) collagen mutations in *Caenorhabditis elegans* and the effects of alpha1 and alpha2(IV) mutations on type IV collagen distribution. J Cell Biol 137:1185–1196. CrossRef Medline

Henderson ST, Gao D, Lambie EJ, Kimble J (1994) lag-2 may encode a signaling ligand for the GLP-1 and LIN-12 receptors of *C. elegans*. Development 120:2913–2924. Medline

Hesselson D, Newman C, Kim KW, Kimble J (2004) GON-1 and fibulin have antagonistic roles in control of organ shape. Curr Biol 14:2005–2010. CrossRef Medline

Hresko MC, Williams BD, Waterston RH (1994) Assembly of body wall muscle and muscle cell attachment structures in *Caenorhabditis elegans*. J Cell Biol 124:491–506. CrossRef Medline

Huang CC, Hall DH, Hedgecock EM, Kao G, Karantza V, Vogel BE, Hutter H, Chisholm AD, Yurchenco PD, Wadsworth WG (2003) Laminin alpha subunits and their role in *C. elegans* development. Development 130:3343–3358. CrossRef Medline

Hutter H, Vogel BE, Plenefisch JD, Norris CR, Proenca RB, Spieth J, Guo C, Mastwal S, Zhu X, Scheel J, Hedgecock EM (2000) Conservation and novelty in the evolution of cell adhesion and extracellular matrix genes. Science 287:989–994. CrossRef Medline

Huxley-Jones J, Robertson DL, Boot-Handford RP (2007) On the origins of the extracellular matrix in vertebrates. Matrix Biol 26:2–11. CrossRef Medline

Hynes RO, Zhao Q (2000) The evolution of cell adhesion. J Cell Biol 150:F89–F96. CrossRef Medline

Ichikawa N, Kasai S, Suzuki N, Nishi N, Oishi S, Fujii N, Kadoya Y, Hatori K, Mizuno Y, Nomizu M, Arikawa-Hirasawa E (2005) Identification of neurite outgrowth active sites on the laminin alpha4 chain G domain. Biochemistry 44:5755–5762. CrossRef Medline

Ihara S, Hagedorn EJ, Morrissey MA, Chi Q, Motegi F, Kramer JM, Sherwood DR (2011) Basement membrane sliding and targeted adhesion remodels tissue boundaries during uterine-vulval attachment in *Caenorhabditis elegans*. Nat Cell Biol 13:641–651. CrossRef Medline

Jin Y (2002) Synaptogenesis: insights from worm and fly. Curr Opin Neurobiol 12:71–79. CrossRef Medline

Jin Y, Jorgensen E, Hartwieg E, Horvitz HR (1999) The *Caenorhabditis elegans* gene unc-25 encodes glutamic acid decarboxylase and is required for synaptic transmission but not synaptic development. J Neurosci 19: 539–548. Medline

Jones G, Meier T, Lichtsteiner M, Witzemann V, Sakmann B, Brenner HR (1997) Induction by agrin of ectopic and functional postsynaptic-like membrane in innervated muscle. Proc Natl Acad Sci U S A 94:2654–2659. CrossRef Medline

Knight D, Tolley LK, Kim DK, Lavidis NA, Noakes PG (2003) Functional analysis of neurotransmission at beta2-laminin deficient terminals. J Physiol 546:789–800. CrossRef Medline

Koushika SP, Richmond JE, Hadwiger G, Weimer RM, Jorgensen EM, Nonet ML (2001) A post-docking role for active zone protein Rim. Nat Neurosci 4:997–1005. CrossRef Medline

Kramer JM (2005) Basement membranes. WormBook, ed. The *C. elegans* Research Community, WormBook, doi/10.1895/wormbook.1.16.1.

Kubota Y, Kuroki R, Nishiwaki K (2004) A fibulin-1 homolog interacts with an ADAM protease that controls cell migration in *C. elegans*. Curr Biol 14:2011–2018. CrossRef Medline

Kubota Y, Nagata K, Sugimoto A, Nishiwaki K (2012) Tissue architecture in the *Caenorhabditis elegans* gonad depends on interactions among fibulin-1, type IV collagen and the ADAMTS extracellular protease. Genetics 190:1379–1388. CrossRef Medline

Mahoney TR, Liu Q, Itoh T, Luo S, Hadwiger G, Vincent R, Wang ZW, Fukuda M, Nonet ML (2006) Regulation of synaptic transmission by RAB-3 and RAB-27 in *Caenorhabditis elegans*. Mol Biol Cell 17:2617–2625. CrossRef Medline

Miner JH, Go G, Cunningham J, Patton BL, Jarad G (2006) Transgenic isolation of skeletal muscle and kidney defects in laminin beta2 mutant mice: implications for Pierson syndrome. Development 133:967–975. CrossRef Medline

Mizoguchi A, Kim S, Ueda T, Kikuchi A, Yorifuji H, Hirokawa N, Takai Y (1990) Localization and subcellular distribution of smg p25A, a ras p21-like GTP-binding protein, in rat brain. J Biol Chem 265:11872–11879. Medline

Mullen GP, Rogalski TM, Bush JA, Gorji PR, Moerman DG (1999) Complex patterns of alternative splicing mediate the spatial and temporal distribution of perlecan/UNC-52 in *Caenorhabditis elegans*. Mol Biol Cell 10:3205–3221. CrossRef Medline

Nishimune H, Sanes JR, Carlson SS (2004) A synaptic laminin-calcium channel interaction organizes active zones in motor nerve terminals. Nature 432:580–587. CrossRef Medline

Noakes PG, Gautam M, Mudd J, Sanes JR, Merlie JP (1995) Aberrant differentiation of neuromuscular junctions in mice lacking s-laminin/laminin beta 2. Nature 374:258–262. CrossRef Medline

Nonet ML (1999) Visualization of synaptic specializations in live *C. elegans* with synaptic vesicle protein-GFP fusions. J Neurosci Methods 89:33–40. CrossRef Medline

Okkema PG, Harrison SW, Plunger V, Aryana A, Fire A (1993) Sequence requirements for myosin gene expression and regulation in *Caenorhabditis elegans*. Genetics 135:385–404. Medline

Palay SL, Chan-Palay V (1976) A guide to the synaptic analysis of the neuropil. Cold Spring Harbor Symp Quant Biol 40:1–16. CrossRef Medline

Pastor-Pareja JC, Xu T (2011) Shaping cells and organs in *Drosophila* by opposing roles of fat body-secreted Collagen IV and perlecan. Dev Cell 21:245–256. CrossRef Medline

Patton BL, Cunningham JM, Thyboll J, Kortesmaa J, Westerblad H, Edström L, Tryggvason K, Sanes JR (2001) Properly formed but improperly localized synaptic specializations in the absence of laminin alpha4. Nat Neurosci 4:597–604. CrossRef Medline

Pöschl E, Schlötzer-Schrehardt U, Brachvogel B, Saito K, Ninomiya Y, Mayer U (2004) Collagen IV is essential for basement membrane stability but dispensable for initiation of its assembly during early development. Development 131:1619–1628. CrossRef Medline

Rogalski TM, Williams BD, Mullen GP, Moerman DG (1993) Products of the unc-52 gene in *Caenorhabditis elegans* are homologous to the core protein of the mammalian basement membrane heparan sulfate proteoglycan. Genes Dev 7:1471–1484. CrossRef Medline

Schwarzbauer JE, Spencer CS (1993) The *Caenorhabditis elegans* homologue of the extracellular calcium binding protein SPARC/osteonectin affects nematode body morphology and mobility. Mol Biol Cell 4:941–952. CrossRef Medline

Sibley MH, Johnson JJ, Mello CC, Kramer JM (1993) Genetic identification, sequence, and alternative splicing of the *Caenorhabditis elegans* alpha 2(IV) collagen gene. J Cell Biol 123:255–264. CrossRef Medline

Sibley MH, Graham PL, von Mende N, Kramer JM (1994) Mutations in the alpha 2(IV) basement membrane collagen gene of *Caenorhabditis elegans* produce phenotypes of differing severities. EMBO J 13:3278–3285. Medline

Siebold B, Qian RA, Glanville RW, Hofmann H, Deutzmann R, Kühn K (1987) Construction of a model for the aggregation and cross-linking region (7S domain) of Type IV collagen based upon an evaluation of the primary structure of the alpha 1 and alpha 2 chains in this region. Eur J Biochem 168:569–575. CrossRef Medline

Singhal N, Martin PT (2011) Role of extracellular matrix proteins and their receptors in the development of the vertebrate neuromuscular junction. Dev Neurobiol 71:982–1005. CrossRef Medline

Somerville RP, Longpre JM, Jungers KA, Engle JM, Ross M, Evanko S, Wight TN, Leduc R, Apte SS (2003) Characterization of ADAMTS-9 and ADAMTS-20 as a distinct ADAMTS subfamily related to *Caenorhabditis elegans* GON-1. J Biol Chem 278:9503–9513. CrossRef Medline

Song S, Zhang B, Sun H, Li X, Xiang Y, Liu Z, Huang X, Ding M (2010) A Wnt-Frz/Ror-Dsh pathway regulates neurite outgrowth in *Caenorhabditis elegans*. PLoS Genet 6:e1001056. CrossRef Medline

Su J, Stenbjorn RS, Gorse K, Su K, Hauser KF, Ricard-Blum S, Pihlajaniemi T, Fox MA (2012) Target-derived matricryptins organize cerebellar synapse formation through alpha3beta1 integrins. Cell Rep 2:223–230. CrossRef Medline

Timpl R, Wiedemann H, van Delden V, Furthmayr H, Kühn K (1981) A network model for the organization of type IV collagen molecules in basement membranes. Eur J Biochem 120:203–211. CrossRef Medline

Vu TH, Werb Z (2000) Matrix metalloproteinases: effectors of development and normal physiology. Genes Dev 14:2123–2133. CrossRef Medline

Wentzel C, Sommer JE, Nair R, Stiefvater A, Sibarita JB, Scheiffele P (2013) mSYD1A, a mammalian synapse-defective-1 protein, regulates synaptogenic signaling and vesicle docking. Neuron 78:1012–1023. CrossRef Medline

White JG, Southgate E, Thomson JN, Brenner S (1986) The structure of the nervous system of the nematode *Caenorhabditis elegans*. Philos Trans R Soc Lond B Biol Sci 314:1–340. CrossRef Medline

Williams BD, Waterston RH (1994) Genes critical for muscle development and function in *Caenorhabditis elegans* identified through lethal mutations. J Cell Biol 124:475–490. CrossRef Medline

Wood WB, Hecht R, Carr S, Vanderslice R, Wolf N, Hirsh D (1980) Parental effects and phenotypic characterization of mutations that affect early development in *Caenorhabditis elegans*. Dev Biol 74:446–469. CrossRef Medline

Wyszynski M, Kim E, Dunah AW, Passafaro M, Valtschanoff JG, Serra-Pagès C, Streuli M, Weinberg RJ, Sheng M (2002) Interaction between GRIP and liprin-alpha/SYD2 is required for AMPA receptor targeting. Neuron 34:39–52. CrossRef Medline

Yurchenco PD (2011) Basement membranes: cell scaffoldings and signaling platforms. Cold Spring Harbor Perspect Biol 3:a004911. CrossRef Medline

Yurchenco PD, Furthmayr H (1984) Self-assembly of basement membrane collagen. Biochemistry 23:1839–1850. CrossRef Medline

Yurchenco PD, Ruben GC (1987) Basement membrane structure in situ: evidence for lateral associations in the type IV collagen network. J Cell Biol 105:2559–2568. CrossRef Medline

Zhen M, Huang X, Bamber B, Jin Y (2000) Regulation of presynaptic terminal organization by *C. elegans* RPM-1, a putative guanine nucleotide exchanger with a RING-H2 finger domain. Neuron 26:331–343. CrossRef Medline